Available online at www.sciencedirect.com

ScienceDirect

Ceramics International 39 (2013) 8641–8647

CERAMICS INTERNATIONAL

www.elsevier.com/locate/ceramint

Synthesis and characterization of copper gallium diselenide powders prepared from the sol–gel derived precursors

Zhi-Liang Liu, Fu-Shan Chen, Chung-Hsin Lu*

Department of Chemical Engineering, National Taiwan University, Taipei, Taiwan, ROC

Received 1 November 2012; received in revised form 11 April 2013; accepted 12 April 2013
Available online 25 April 2013

Abstract

Copper gallium diselenide ($CuGaSe_2$) powders were synthesized via the sol–gel method followed by a selenization process. The sol–gel process can effectively reduce the required synthesis temperature to 400 °C due to enhanced reactivity and improved composition homogeneity. The amount of Cu_2Se impurity phase was decreased when sufficient Ga^{3+} was added to the precursors. $CuGaSe_2$ powders were successfully prepared when the Ga^{3+}/Cu^{2+} molar ratio was increased to 2. The formation of $CuGaSe_2$ with a pure chalcopyrite structure was confirmed via the Rietveld refinement analysis. With decreasing Ga^{3+}/Cu^{2+} molar ratios, the particle size of the prepared $CuGaSe_2$ powders was significantly enlarged because the copper selenide phase acted as a flux for the particle growth. The optical absorption spectra revealed the obtained $CuGaSe_2$ to have a band gap of 1.68 eV. The sol–gel method combined with the selenization process was demonstrated to provide a potential approach for fabricating $CuGaSe_2$ materials.

Keywords: A. Sol–gel processes; Chalcopyrite; $CuGaSe_2$

1. Introduction

Thin-film solar cells have been developed as the second-generation solar cells because the absorption materials are cost effective. Because of the direct band gap and high absorption coefficient, chalcopyrite semiconductors are considered to be the promising candidates for thin-film solar cells. $Cu(In,Ga)Se_2$ (CIGS) with a CIGS/CdS/ZnO junction was demonstrated to exhibit high efficiency as reported by NREL and ZSW [1,2]. For further improving the efficiency, the tandem-structure solar cells connect two cells in series. The bottom and top cells absorb the red and blue sunlight portion, respectively. The chalcopyrite material $CuGaSe_2$ (CGS) with a large band gap is considered as a potential material for the top cell in multi-junction devices [3]. It has been reported that a tandem structure with CGS as the top cell and CIGS as the bottom cell can increase the conversion efficiency [4].

CGS and CIGS based absorbers are usually obtained via the vacuum routes [5–7]. However, the conventional vacuum systems have several drawbacks including the high production costs, difficulty in scaling up, and process complexity. Because of its' relatively simple procedure, low cost, and flexibility in scaling up [8,9], a particle based coating process is considered as an alternate process for CGS and CIGS absorber films.

CGS and CIGS powders are usually synthesized via the solvo-thermal [10,11] or solid-state process [12]. The required reaction temperature in the solid state process is at least 800 °C to form the pure phase [13]. In addition, the particle size of CGS and CIGS is difficult to control via the solid-state process. In the particle-based process, the particle sizes of CGS significantly affect the morphology and the surface state of absorption films. Hence, the way to control the particle size is important in particle-based deposition methods. To reduce the reaction time and temperatures, a sol–gel method utilizing polymerizing agents followed by a selenization process was used in this study. The molar ratios of Ga^{3+} to Cu^{2+} in the precursor of CGS powders were modified to form the pure phase and control the morphology.

*Corresponding author. Tel.: +886 2 23651428; fax: +886 2 23623040.
E-mail addresses: chlu@ntu.edu.tw, chlu@ccms.ntu.edu.tw (C.-H. Lu).

0272-8842/$ - see front matter © 2013 Elsevier Ltd and Techna Group S.r.l. All rights reserved.
http://dx.doi.org/10.1016/j.ceramint.2013.04.042

2. Experimental

$CuGaSe_2$ powders were prepared via the sol–gel route employing citric acid and ethylene glycol as the polymerizing agents. Copper nitride and gallium nitride were dissolved in deionized water. The molar ratios of $Cu(NO_3)_2$ to $Ga(NO_3)_3$ were varied from 1:1 to 1:2. Afterward, citric acid was added in the solution. After stirring for 1 h, ethylene glycol was then added into the mixed solution. The mixed solution was stirred and heated at 100 °C for 1 h to remove the excess water, followed by increasing the temperature to 200 °C to initiate the polymerization reaction. During the polymerization reaction, citric acid was used to chelate the metal ions and polymerize with ethylene glycol to form the gels. The brownish gels were formed after the polymerization reaction. To remove the organic residuals, the brownish gels were heated in air at 420 °C for 2 h. After the heating process, the precursors were formed. The precursors were selenized at temperatures ranging from 450 °C to 550 °C using a gas mixture (5 vol% H_2 and 95 vol% N_2) with selenium vapor to form $CuGaSe_2$ particles.

The phases of the prepared samples were examined using an X-ray diffractometer (XRD, Philips X' Pert/MPD, Tokyo, Japan) using CuKα radiation at 45 kV and 40 mA. The morphology of the $CuGaSe_2$ powders was observed using a scanning electron microscope (SEM, Hitachi S-800, Tokyo, Japan). The band gap of the $CuGaSe_2$ particles was measured using a UV/vis/NIR spectrophotometer (UV, Jasco V-570). The prepared products were characterized via X-ray photoelectron spectra (XPS, VG Scientific ESCALAB 250, UK).

3. Results and discussion

3.1. Compositional effects on the formation and morphology of $CuGaSe_2$ powders via the sol–gel route

The $CuGaSe_2$ sol–gel derived precursors were selenized at different reaction temperatures for 1 h. The Ga^{3+}/Cu^{2+} molar ratio was set to 1. Fig. 1 illustrates the X-ray diffraction patterns of the precursors and resultant compounds. CuO and Ga_2O_3 phases were observed in the sol–gel derived precursors as shown in Fig. 1(a). After selenization at 450 °C, the phase of $CuGaSe_2$ started to form (Fig. 1(b)). In addition, a small amount of Cu_2Se was found to coexist with $CuGaSe_2$. As the reaction temperature was increased to 500 °C and 550 °C (Fig. 1(c) and (d)), the amount of $CuGaSe_2$ increased monotonously. However, the impurity phase of Cu_2Se remained to coexist with $CuGaSe_2$ in the samples. The formation of Cu_2Se implies that the Ga species were insufficient during the reactions.

The precursors of $CuGaSe_2$ were selenized to form $CuGaSe_2$ powders. A reducing atmosphere (5% H_2 and 95% N_2) was used during the selenization process. The hydrogen gas caused the reduction of Ga_2O_3 (Fig. 1(a)) to form Ga metal. The metallic gallium is easily vaporized because of the low melting point of Ga metal (29.7 °C). The evaporation of gallium species will result in the gallium loss in the selenization process. In order to compensate for the gallium loss and supply

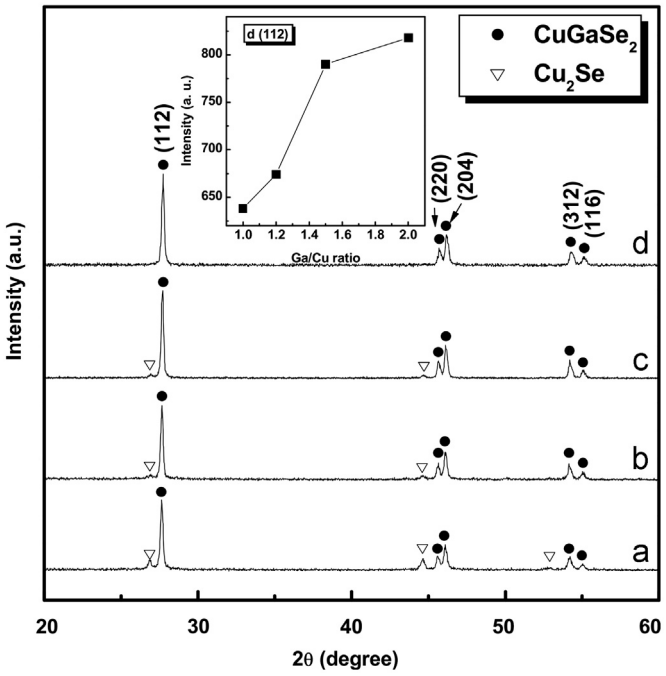

Fig. 1. XRD patterns of $CuGaSe_2$ powders prepared with the Cu^{2+} to Ga^{3+} molar ratio of 1.0 at (a) precursor, (b) 450 °C, (c) 500 °C, and (d) 550 °C for 1 h in the sol–gel process.

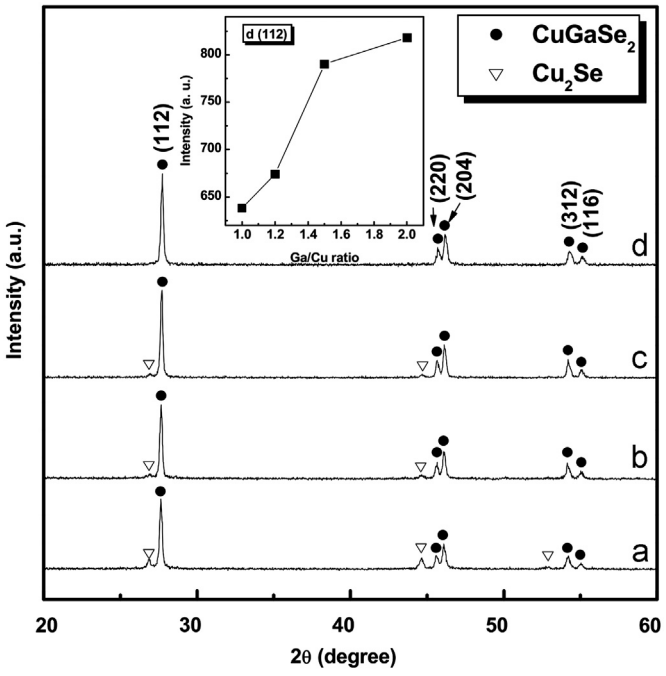

Fig. 2. XRD patterns of $CuGaSe_2$ powder prepared at 550 °C for 1 h with the Ga^{3+} to Cu^{2+} molar ratios of (a) 1.0, (b) 1.2, (c) 1.5, and (d) 2.0 in the sol–gel process. Inset: the relation between the Ga^{3+}/Cu^{2+} molar ratios and the diffraction peak intensity of $CuGaSe_2$.

sufficient Ga during the reactions, the Ga^{3+}/Cu^{2+} molar ratio in the precursors should be increased.

To investigate the effects of Ga^{3+}/Cu^{2+} molar ratio on the formed phase, the Ga^{3+}/Cu^{2+} molar ratio was varied to 1, 1.2,

1.5 and 2. The prepared $CuGaSe_2$ precursors were selenized at 550 °C for 1 h. The X-ray diffraction patterns of the obtained powders are illustrated in Fig. 2. When the Ga^{3+}/Cu^{2+} molar ratio was 1 (Fig. 2(a)), $CuGaSe_2$ was formed with a large amount of Cu_2Se. As the Ga^{3+}/Cu^{2+} molar ratio was increased to 1.2 and 1.5 (Fig. 2(b) and (c)), the amount of Cu_2Se decreased. When the Ga^{3+}/Cu^{2+} molar ratio was adjusted to 2.0, the single-phased $CuGaSe_2$ powders were successfully prepared (Fig. 2(d)).

In comparison with the solid state processes [13], the preparation temperatures for $CuGaSe_2$ were significantly reduced when the sol–gel method and the selenization process were utilized. The sol–gel route using polymerizing agents leads to the formation of tiny gel cages during polymerization [14,15]. The immobilization of metal–ion complexes in the tiny gel cages results in improvement in the compositional homogeneity. Hence, the reactivity of reactant was increased and the preparation temperatures were decreased via the sol–gel route. The obtained XRD pattern was consistent with the chalcopyrite structure phase of $CuGaSe_2$ (ICDD card no. 75-0104). The relation between the Ga^{3+}/Cu^{2+} molar ratios and the diffraction peak intensity of $CuGaSe_2$ is depicted in the inset of Fig. 2. The results shown in Fig. 2 indicate that the molar ratios between Ga^{3+} and $Cu^{2/+}$ significantly influenced the formation of $CuGaSe_2$. The single-phased $CuGaSe_2$ was formed when sufficient gallium ions were supplied during the reactions. The pure $CuGaSe_2$ phase was obtained when the Ga^{3+}/Cu^{2+} molar ratio was 2. Therefore, the Ga^{3+}/Cu^{2+} molar ratio was fixed at 2 in the following experiments.

The SEM micrographs of the 550 °C-heated sample with different Ga^{3+}/Cu^{2+} molar ratios are shown in Fig. 3. The prepared powders exhibited a typical particulate morphology. When the Ga^{3+}/Cu^{2+} molar ratio was 1, the particle size of the sample was around 330 nm, as seen in Fig. 3(a). When the Ga^{3+}/Cu^{2+} molar ratio was increased to 1.2, the particle size of the obtained powder was around 180 nm (Fig. 3(b)). As the Ga^{3+}/Cu^{2+} molar ratios further raised to 1.5 and 2.0, the particle sizes were around 90 nm and 70 nm (Fig. 3(c) and (d)), respectively. It is found that the particle size of $CuGaSe_2$ was decreased with increasing Ga^{3+}/Cu^{2+} molar ratios. When the Ga^{3+}/Cu^{2+} molar ratio is low, the Cu–Se phases will segregate in the samples and act as a flux at elevated

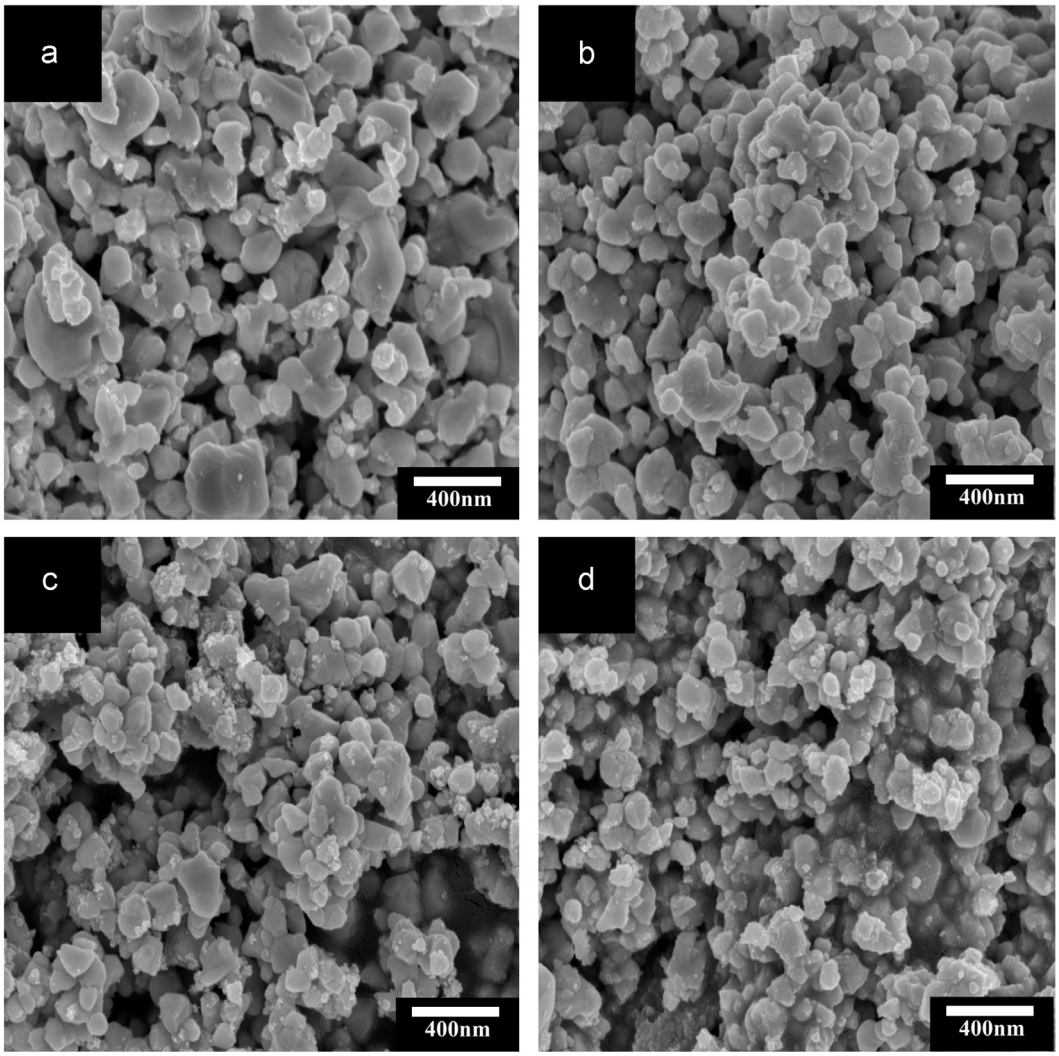

Fig. 3. SEM micrographs of $CuGaSe_2$ powders selenized at 550 °C for 1 h with the Ga^{3+}/Cu^{2+} molar ratios of (a) 1, (b) 1.2, (c) 1.5 and (d) 2.

temperatures to promote the grain growth and enlarge $CuGaSe_2$ particles [16–18].

3.2. Characterization of $CuGaSe_2$ powders

For analyzing the crystal structure of the prepared $CuGaSe_2$ powders, the Rietveld refinement method was employed to identify the crystal system, space group and lattice constant of the obtained particles. Fig. 4 shows the refined XRD patterns of the prepared powders. The "x" marks and solid curves represent the experimental diffraction data and the simulated diffraction data, respectively. The straight bars indicate the position of the simulated diffraction data. The dotted lines show the deviation between the simulated and experimental values. The refinement results of $CuGaSe_2$ are listed in Table 1. The reliability factors R_{wp} and R_p are 5.94% and 4.65%, respectively. Based on the reliability factors, the refinement results provide reliable values for the prepared samples. The lattice constants of a and c are 5.602 Å and 11.000 Å, respectively. It was found that the lattice parameter η ($\eta = c/2a$) was 0.982 deviated from 1. It is because of the unequal bond lengths of Cu–Se and Ga–Se in the chalcopyrite structure [19]. All structural parameters and the refinement results are in agreement with the JCPD files [20].

To determine the band gap of $CuGaSe_2$, the optical properties of the prepared powders were examined via UV–Vis–NIR spectrometer. The band gap of the $CuGaSe_2$ samples was calculated from the optical absorption data according to the equation as illustrated below [21]:

$$\alpha\nu h = k(h\nu - E_G)^{1/2}$$

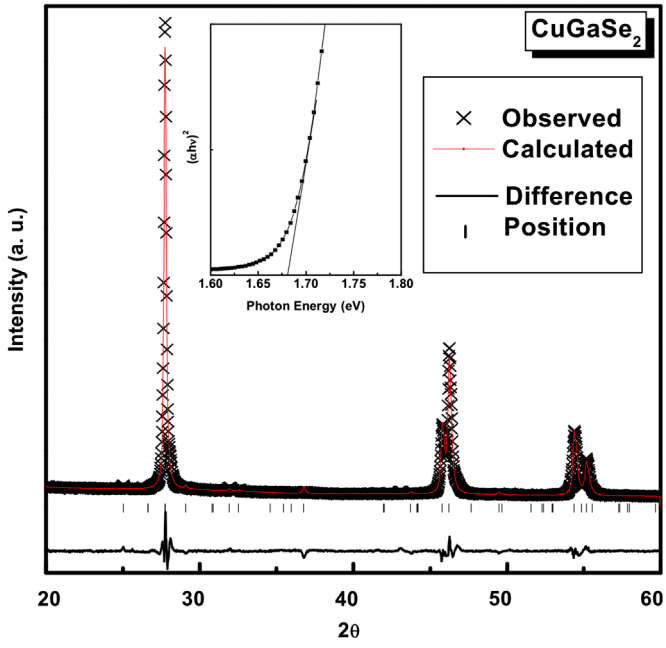

Fig. 4. Observed (×) and calculated (upper solid line) X-ray diffraction patterns of $CuGaSe_2$ powders with difference profile (lower solid line) and positions of all the reflections (vertical bars). Inset: the UV–Vis–NIR spectra of $CuGaSe_2$ powders.

Table 1
Rietveld refinement calculations of $CuGaSe_2$.

Formula	$CuGaSe_2$
Crystal system	Tetragonal
Space group	I-42d
Lattice constants	
a (Å)	5.602
c (Å)	11.000
$\eta = c/2a$	0.982
Cell volume, V (Å^3)	345.171
R values	R_{wp}=5.94%
	R_p=4.65%

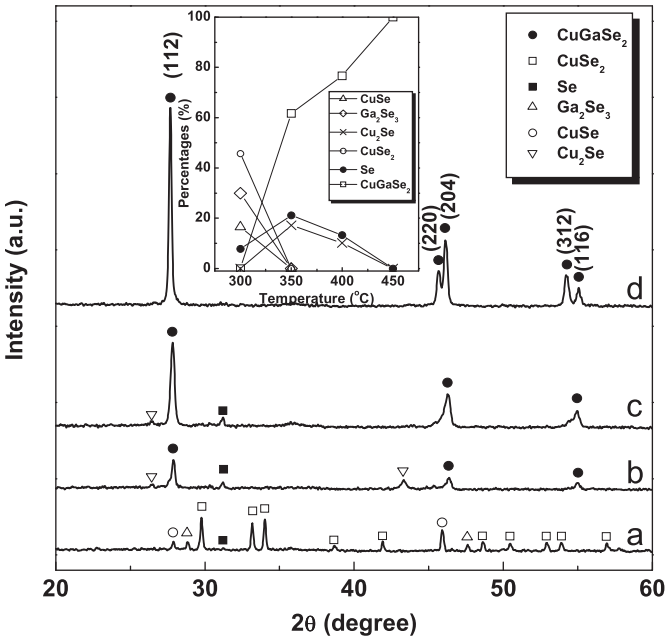

Fig. 5. XRD patterns of $CuGaSe_2$ powders selenized at (a) 300 °C, (b) 350 °C, (c) 400 °C, and (d) 450 °C for 40 min in the sol–gel process. Inset: the relation between the fraction of the resultant compounds and the reaction temperatures.

where α is the absorption coefficient, k is constant, $h\nu$ is the photon energy and E_G is the band gap energy. The band gap was measured via plotting an $(\alpha h\nu)^2$ versus $h\nu$. The extrapolation of the dash line in the graph to $(\alpha h\nu)^2 = 0$ gives the energy band gap value. As shown in the inset of Fig. 4, the absorption measurement indicates that the optical band gap of obtained $CuGaSe_2$ powder was 1.68 eV, which is consistent with the data reported in the literature [22].

3.3. Effects of the reaction conditions on the formation of $CuGaSe_2$ powders

The selenization process was carried out at different reaction temperatures for 40 min with the Ga^{3+}/Cu^{2+} molar ratio fixed at 2. Fig. 5 illustrates the X-ray diffraction patterns of the obtained powders. The relation between the fraction of the resultant compounds and the reaction temperatures is depicted in the inset of Fig. 5. After heating at 300 °C (Fig. 5(a)), Se, CuSe, Ga_2Se_3 and $CuSe_2$ were observed. As the reaction

temperature was increased to 350 °C, CuSe and $CuSe_2$ phases completely disappeared and Cu_2Se was formed (Fig. 5(b)). Upon heating to 400 °C, $CuGaSe_2$ started to form. However, a small amount of selenium and Cu_2Se was found to exist along with $CuGaSe_2$ (Fig. 5(c)). When the temperature was increased to 450 °C, pure $CuGaSe_2$ was obtained (Fig. 5(d)).

To realize the phase change of copper selenides during the reaction, the oxidation states of selenium were analyzed via XPS. The Se3d XPS spectra of the samples heated at 300 °C, 400 °C and 450 °C are shown in Fig. 6(a)–(c), correspondingly. As shown in Fig. 6(a), the peak was deconvoluted into two peaks. The two peaks observed at 54.8 eV and 55.6 eV indicate that the 300 °C-heated sample included selenium in the form of CuSe [23] and Se^0 [24], respectively. The peak for the 400 °C-heated sample was deconvoluted into four peaks in the range from 53.3 eV to 55.3 eV (Fig. 6(b)). These four peaks indicate the existence of the Se^0, Cu_2Se and $CuGaSe_2$ phases [24,25]. As for the 450 °C-heated sample, only two peaks of $CuGaSe_2$ phase were observed without the existence of the peaks of Se^0 and Cu_2Se (Fig. 6(c)). The above results show that the Se3d signals change from Se^0 at 300 °C to Se^{2-} at 450 °C. The change in the selenium oxidation states is consistent with the data shown in Fig. 5.

For investigating the influence of reaction time on the formation of resultant phases, the selenization process was carried out at 400 °C for various selenization durations. The X-ray diffraction patterns of the samples are illustrated in Fig. 7. After heating for 20 and 40 min (Fig. 7(a) and (b)), unreacted Cu_2Se and selenium were found to coexist with $CuGaSe_2$, implying that the reaction was not complete. As the duration was prolonged to 80 and 120 min (Fig. 7(c) and (d)), pure $CuGaSe_2$ was obtained. The crystallinity of $CuGaSe_2$ was enhanced when the reaction time was raised.

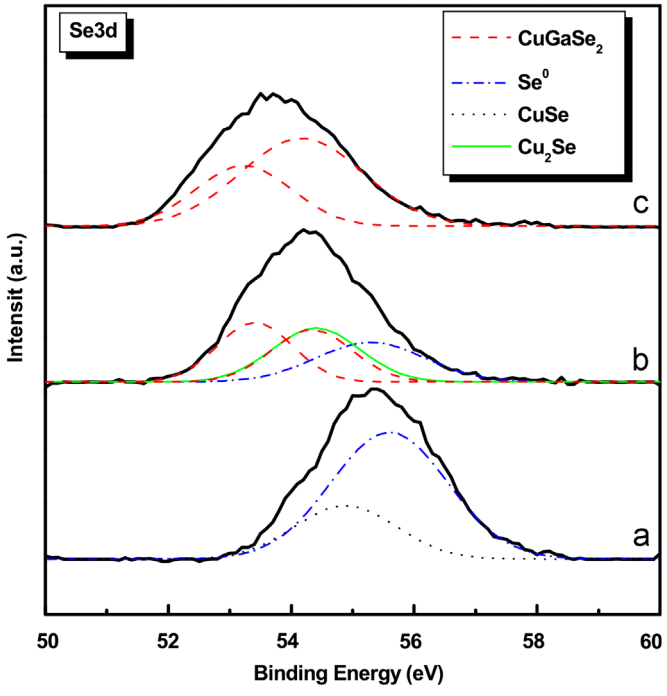

Fig. 6. Se3d spectra of $CuGaSe_2$ precursor powders selenization at (a) 300 °C, (b) 400 °C, and (c) 450 °C.

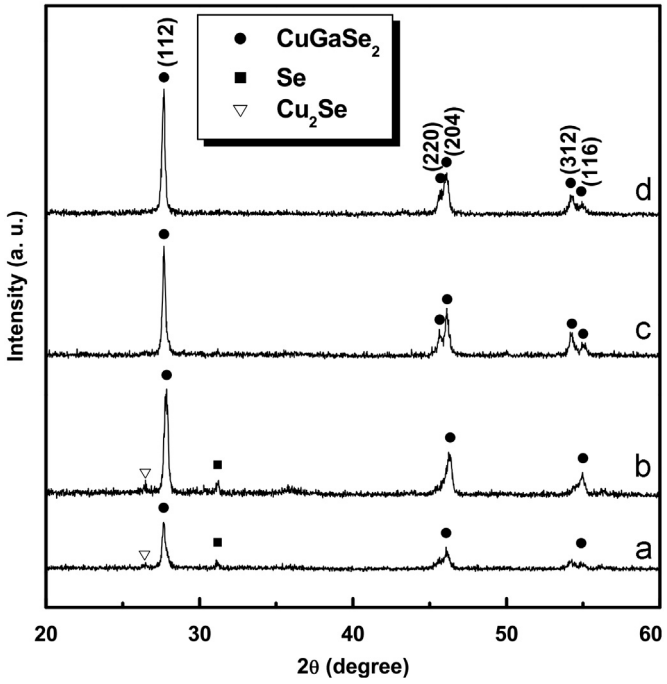

Fig. 7. XRD patterns of $CuGaSe_2$ powders selenized at 400 °C with the Ga^{3+}/Cu^{2+} molar ratio of 2 for (a) 20 min, (b) 40 min, (c) 80 min, and (d) 120 min in the sol–gel process.

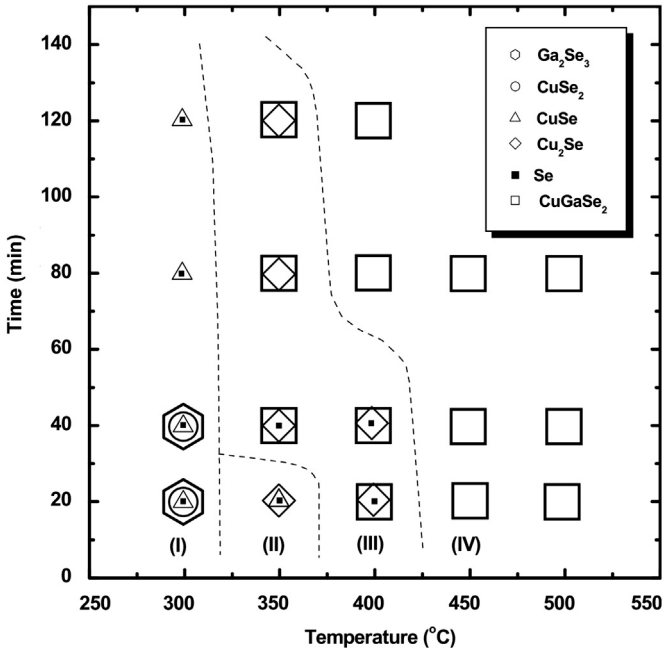

Fig. 8. Resultant compounds of $CuGaSe_2$ precursors selenized with different heating conditions.

The sol–gel derived precursors of $CuGaSe_2$ were selenized at different reaction temperatures and reaction durations. The resultant compounds prepared under different reaction

conditions are illustrated in Fig. 8. Based on the formed phases, this figure can be divided into four major zones. In zone I, as the reaction temperature is comparatively low and the reaction time is short, CuSe and selenium are formed as the main phases. With increasing the reaction temperatures at short reaction durations, the Cu_2Se phase is formed in zone II. In this region, a small amount of selenium is also observed. As the reaction temperatures are further raised or the reaction time is prolonged, the $CuGaSe_2$ phase is formed in zone III. The impurity phases of selenium and Cu_2Se are also observed in this region. Further increasing the reaction time or increasing the reaction temperature causes the formation of single-phased $CuGaSe_2$, as shown in zone IV. The above results indicate that CuSe and Cu_2Se are the major intermediate compounds existing in the reaction process. It is implied that increasing the reactivity of the Cu–Se compounds with the constituent species can facilitate the formation of $CuGaSe_2$ powders. When the samples are heated at 400 °C, the pure phase is obtained after heating for 80 min. As the samples are heated at 450 °C, the pure phase is achieved after heating for 20 min. Increasing the heating temperatures can shorten the required heating time for obtaining the pure $CuGaSe_2$ phase.

4. Conclusions

$CuGaSe_2$ powders were successfully synthesized via the sol–gel route followed by a selenization process in a reducing atmosphere. As the Ga^{3+}/Cu^{2+} molar ratio was increased, the amounts of the impurity phase Cu_2Se were reduced. When the Ga^{3+}/Cu^{2+} molar ratio was adjusted to 2, the single-phased $CuGaSe_2$ was obtained after heating at 400 °C for 80 min. In comparison with the solid-state process, the reaction temperature for preparing $CuGaSe_2$ was significantly reduced via the sol–gel route due to the reducing segregation of metal ions in the polymerization process. The Rietveld refinement analysis confirmed the formation of $CuGaSe_2$ with a pure chalcopyrite structure. The particle sizes of $CuGaSe_2$ were increased with decreasing Ga^{3+}/Cu^{2+} molar ratios because the Cu–Se phases acted as the flux for the particle growth. The optical absorption revealed that the obtained $CuGaSe_2$ had a band gap of 1.68 eV. The sol–gel route with a selenization process was demonstrated to be a potential approach for synthesizing pure $CuGaSe_2$ powders.

Acknowledgments

The authors would like to thank the National Science Council, Taiwan, the Republic of China, for partial financial support of this study under Contract no. NSC 100-3113-E002-011.

References

[1] M. Bär, I. Repins, M.A. Contreras, L. Weinhardt, R. Noufi, C. Heske, Chemical and electronic surface structure of 20%-efficient Cu(In,Ga)Se_2 thin film solar cell absorbers, Applied Physics Letters 95 (2009) 052106.

[2] P. Jackson, D. Hariskos, E. Lotter, S. Paetel, R. Wuerz, R. Menner, W. Wischmann, M. Powalla, New world record efficiency for Cu(In,Ga)Se_2 thin-film solar cells beyond 20%, Progress in Photovoltaics 19 (2011) 894.

[3] T.J. Coutts, K.A. Emery, J.S. Ward, Modeled performance of polycrystalline thin-film tandem solar cells, Progress in Photovoltaics: Research and Applications 10 (2002) 195.

[4] S. Nishiwaki, S. Siebentritt, P. Walk, A stacked chalcopyrite thin-film tandem solar cell with 1.2 V open-circuit voltage, Progress in Photovoltaics: Research and Applications 11 (2003) 243.

[5] A. Hultqvist, C.P. Björkman, J. Pettersson, T. Törndahl, M. Edoff, $CuGaSe_2$ solar cells using atomic layer deposited Zn(O,S) and (Zn,Mg)O buffer layers, Thin Solid Films 517 (2009) 2305.

[6] V. Probst, J. Palm, S. Visbeck, T. Niesen, R. Tölle, A. Lerchenberger, M. Wendl, H. Vogt, H. Calwer, W. Stetter, F. Karg, New developments in Cu(In,Ga)(S, $Se)_2$ thin film modules formed by rapid thermal processing of stacked elemental layers, Solar Energy Materials and Solar Cells 90 (2006) 3115.

[7] L.C. Yang, C.Y. Cheng, J.S. Fang, Characterization of polycrystalline $CuInSe_2$ thin films deposited by sputtering and evaporation as a function of composition, Journal of Physics and Chemistry of Solids 69 (2008) 435.

[8] M. Kaelin, D. Rudmann, A.N. Tiwari, Low cost processing of CIGS thin film solar cells, Solar Energy 77 (2004) 749.

[9] C. Eberspacher, C. Fredric, K. Pauls, J. Serra, Thin-film CIS alloy PV materials fabricated using non-vacuum, particles-based techniques, Thin Solid Films 387 (2001) 18.

[10] C.H. Lee, C.H. Wu, C.H. Lu, Microwave-assisted solvothermal synthesis of copper indium diselenide powders, Journal of the American Ceramic Society 93 (2010) 1879.

[11] C.H. Lu, C.H. Lee, C.H. Wu, Microemulsion-mediated solvothermal synthesis of copper indium diselenide powders, Solar Energy Materials and Solar Cells 94 (2010) 1622.

[12] K. Yoshino, M. Sugiyama, D. Maruoka, S.F. Chichibu, H. Komaki, K. Umeda, T. Ikari, Photoluminescence spectra of $CuGaSe_2$ crystals, Physica B 302–303 (2001) 357.

[13] L.S. Lerner, A $CuGaSe_2$ and $GiNSe_2$: preparation and properties of single crystals, Journal of Physics and Chemistry of Solids 27 (1966) 1.

[14] C.H. Hsu, C.L. Liaw, C.H. Lu, Luminescence properties of sol–gel derived $Sr_2(Ce_{1-x}Sn_x)O_4$ blue phosphors, Journal of Alloys and Compounds 489 (2010) 445.

[15] C.H. Lu, W.T. Hsu, B.M. Cheng, Luminescence characteristics of sol–gel derived $Y_3Al_5O_{12}$: Eu^{3+} phosphors excited with vacuum ultraviolet, Journal of Applied Physics 100 (2006) 063535.

[16] I. Repins, M.A. Contreras, B. Egaas, C. DeHart, J. Scharf, C.L. Perkins, B. To, R. Noufi, 19.9%-efficient ZnO/CdS/$CuInGaSe_2$ solar cell with 81.2% fill factor, Progress in Photovoltaics: Research and Applications 16 (2008) 235.

[17] J. Kessler, C. Chityuttakan, J. Schöldström, L. Stolt, Growth of Cu(In,Ga)Se_2 films using a Cu-poor/rich/poor sequence: substrate temperature effects, Thin Solid Films 431–432 (2003) 1.

[18] S. Merdes, A. Kinoshita, Z. Hadjoub, M. Sugiyama, H. Nakanishi, H. Nakanishi, S. Ando, Effect of alternating Cu poor/Cu rich/Cu poor/Cu rich/layers of metal naphthenates in the growth process on the properties of $CuInSe_2$ thin films prepared by the spin coating technique, Thin Solid Films 516 (2008) 7335.

[19] T. Todorov, D.B. Mitzi, Direct liquid coating of chalcopyrite light-absorbing layers for photovoltaic devices, European Journal of Inorganic Chemistry 1 (2010) 17.

[20] Powder Diffraction File, Joint Committee on Powder Diffraction Standards, Swarthmore.

[21] L. Oliveira, T. Todorov, E. Chassaing, D. Lincot, J. Carda, P. Escribano, CIGSS films prepared by sol–gel route, Thin Solid Films 517 (2009) 2272.

[22] F.J. Haug, M. Krejci, H. Zogg, A.N. Tiwari, M. Kirsch, S. Siebentritt, Characterization of $CuGa_xSe_y$/ZnO for superstrate solar cells, Thin Solid Films 361–362 (2000) 239.

[23] Y. Zhang, Z.P. Qiao, X.M. Chen, Microwave-assisted elemental direct reaction route to nanocrystalline copper chalcogenides CuSe and Cu_2Te, Journal of Materials Chemistry 12 (2002) 2747.

[24] R. Würz, M. Rusu, Th. Schedel-Niedrig, M.Ch. Lux-Steiner, H. Bluhm, M. Hävecker, E. Kleimenov, A. Knop-Gericke, R. Schlögl, In situ X-ray photoelectron spectroscopy study of the oxidation of $CuGaSe_2$, Surface Science 580 (2005) 80.

[25] A.B.M.O. Al-Mamun, A.H.Bhuiyan Islam, Structural, electrical and optical properties of copper selenide thin films deposited by the chemical bath deposition technique, Journal of Materials Science: Materials in Electronics 16 (2005) 263.